Aircraft Data and Flux Calculation Technique

1. Aircraft Data

Aircraft data were collected at 25 Hz using the University of Wyoming King Air gust-probe aircraft. Data were recorded at 25 Hz. Both One-Hz and 25-Hz data are available at http://kingair.uwyo.edu/projects/ihop02/data/. Below we list the data used for fluxes.

Figure 1. University of Wyoming King Air. Photo courtesy of Bob McMillan, NOAA

- **Aircraft position (LAT, LON) and motion relative to the ground** were measured by a Honeywell Laseref SM inertial navigation system and corrected using GPS. Aircraft position is correct to within 100 m horizontally (Al Rodi, personal communication, 2006), so that rstb, ndvi, and aircraft video images could easily be correlated with surface features. A reverse flow thermometer measured air temperature, and a Heiman KT-19.85 radiometer sensed T_s.
- **Aircraft altitude**
  - King KRA5 radar altimeter for heights below 610 m (ralt1)
  - APN159 radar altimeter for heights above 610 m (ralt2)
  - Pressure altitude (ztrue)
- **Air velocity components** for fluxes and mean winds: hu (positive east), hv (positive north), hw (positive up)
- **Mixing ratio (for fluxes)**

- LiCor 6262 gas analyzer (h2omx)
- Lyman-alpha (mrla, mrlaf)

- **Air Temperature**
  - Potential temperature for fluxes (thetad) was calculated from the pressure from a Rosemount 1201 sensor and air temperature from a reverse-flow thermometer
- **Air Density** (for conversion of fluxes to H and LE)
  - Air temperature (Trose) from a Rosemont 102 sensor
  - Air pressure (pmb) Rosemont 102F1B4A1A
  - Mixing ratio (h2omx)
- **Radiometric Surface Temperature** (rstb) Heiman KT-19.85 radiometer
- **Normalized Differential Vegetation Index** (ndvi) was estimated from an Exotech radiometer, from $NDVI = \frac{r_4 - r_3}{r_4 + r_3}$,where r_4 is the amount of electromagnetic radiation reflected in the near-infrared at 0.762-0.898 μm, and r_3 is the amount of electromagnetic radiation reflected in the red at 0.629-0.687 μm.

Figure 2 shows the three tracks used for IHOP_2002 Boundary Layer Heterogeneity (BLH) missions, which were designed to document the effects of the surface on BL thermodynamic fluxes and structure. The flight-track locations extended from the Oklahoma Panhandle to south-eastern Kansas, to sample a large range of precipitation, soils, and land cover types. From Table 1, the Eastern Track has green and dense vegetation (average NDVI~0.6), cooler T_s, and higher rainfall than the Western Track (average NDVI 0.1-0.2). The Central Track has intermediate characteristics.

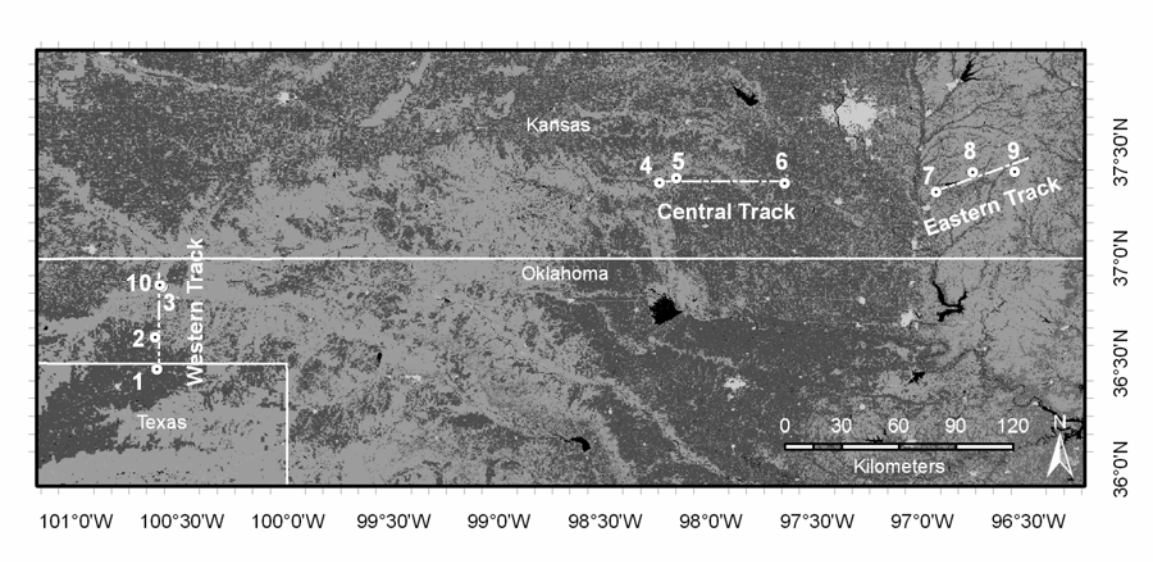

Figure 2. Locations of Boundary Layer Heterogeneity (BLH) flight tracks. Numbers denote surface flux stations. Sites 1-9 are NCAR/ISFF sites; Site 10 was operated by the University of Colorado. Darker color: Row crops (mostly winter wheat); lighter color: grasslands; black: water.

Each IHOP Boundary Layer Heterogeneity (BLH) King-Air mission consisted of multiple straight-and-level legs along a single track, interspersed with soundings to check mixed-layer depth (as defined by near-constant potential temperature Θ) depth. Some legs were always flown at 70 m above ground level (agl), with at least one other height within the BL represented. The flight pattern changed with the research emphasis, with more 70-m legs for flux missions, and legs divided more evenly between 2-4 heights for BL structure missions. The lowest legs (below 100-150 m) were flown at a roughly constant height above the ground (see Fig. 3 for elevation along the tracks), while the higher legs were flown according to pressure altitude, so that altitude above the ground varied around the specified leg height.

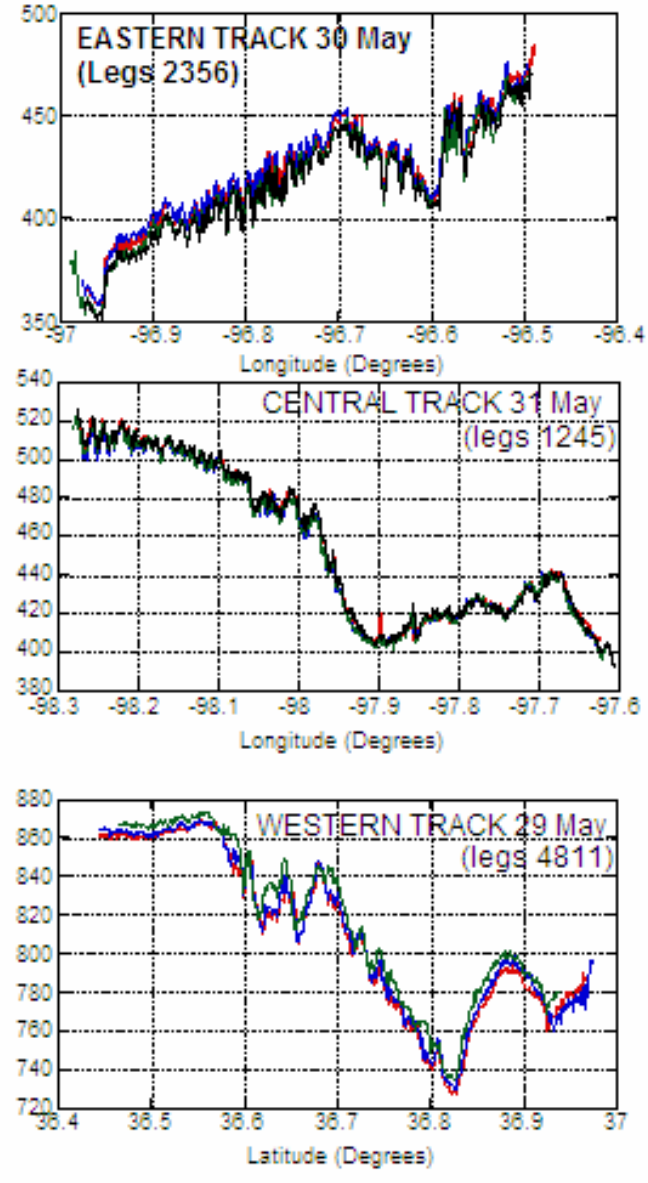

Figure 3: Elevations along the three flight tracks

2. Flux calculation

"Total" grand-average IHOP_2002 and CASES-97 fluxes along the Eastern Track for a given day were calculated in a multiple-step procedure following LeMone et al. (2003).

a. Time series for potential temperature Θ, mixing ratio Q, and vertical velocity W for each leg were detrended by subtracting out the best-fit line based on linear regression.
b. Data were time-shifted because of horizontal displacement and differences in response time between vertical velocity and the temperature and humidity sensors
    - Licor mixing ratio (h2omx) is shifted 0.32 s (8 points) earlier
    - Lyman-alpha (mrla) is shifted 0.08 s (4 points) earlier (following Kang et al. 2006)
    - Thetad is shifted 0.08 s (4 points) earlier
    a. The resulting time series ($\theta(t)$, $q(t)$, and $w(t)$) are multiplied to form $\theta(t)w(t)$ and $q(t)w(t)$ time series.
    b. Leg times adjusted so that the west or south end is at a common point.
    c. $\theta(t)w(t)$ and $q(t)w(t)$ are averaged into 1-km increments, based on 1-s "slow" LAT and LON.
    d. If step b not completed, data interpolated to common points.
    e. The 1-km data for each leg are smoothed using a 4-km running-mean average.
    f. The smoothed fluxes at corresponding points were averaged to form the grand average leg.

3. Evaluation of the Data

a. Comparison with "high-frequency" fluxes

We chose to estimate fluxes relative to leg linear trends to maximize agreement with surface data and because it allows easy flexibility in choosing a filter once the 1-km data are processed. In contrast to Kang et al. (2006), who calculate 4-km fluxes for the IHOP_2002 Western Track relative to the corresponding 4-km means. To contrast the two approaches directly, we calculated fluxes relative to 1-km averages and then smoothed the resulting data using a 4-point filter ("high-frequency" fluxes). The fluxes from the "total flux" (leg linear trends subtracted out), in Figure 4 are qualitatively quite similar to those from the high-frequency fluxes in Figure 5, an encouraging result.

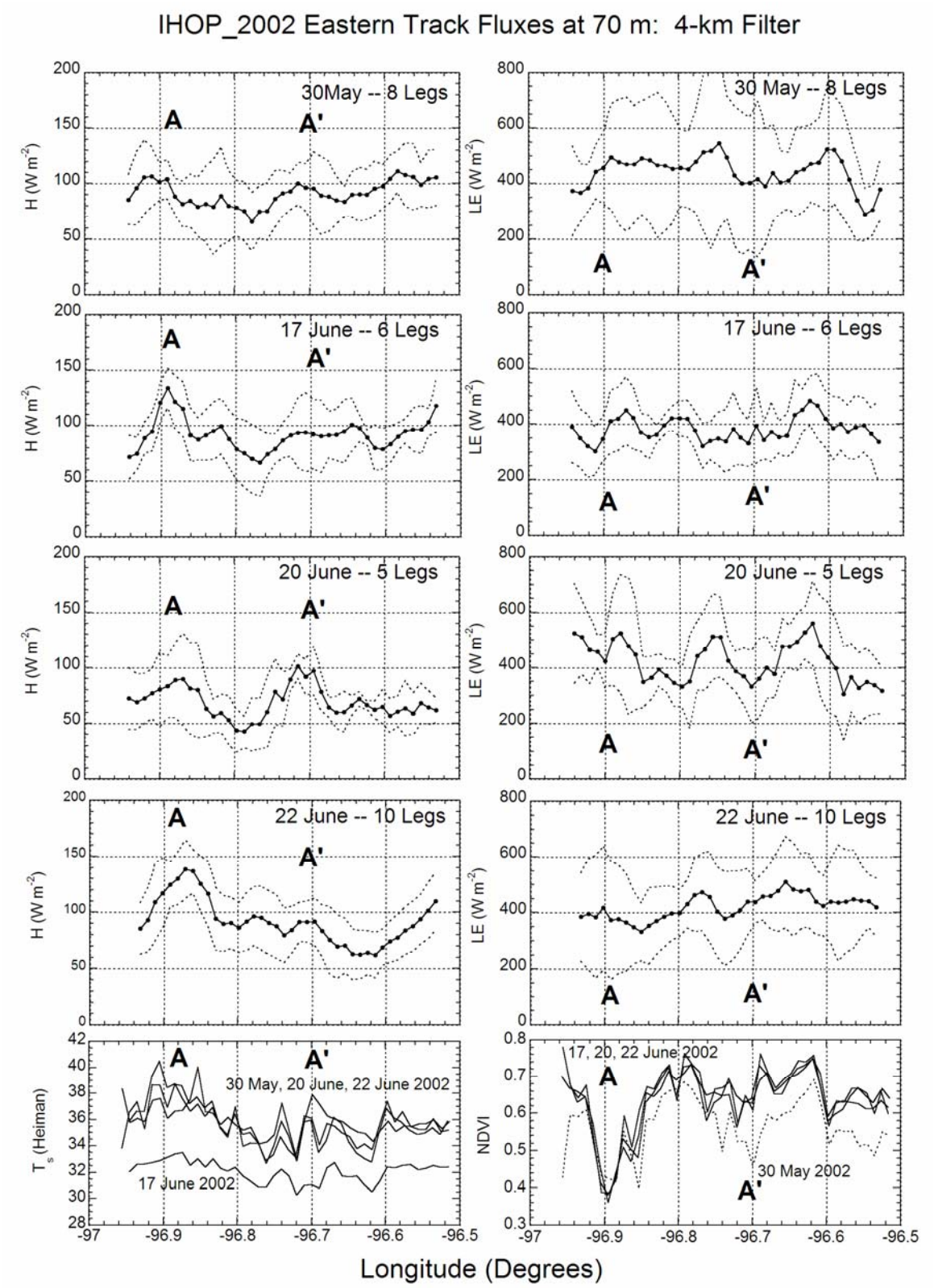

Figure 4. "Total" sensible heat flux H and latent heat LE with standard deviations for the grand average legs for four missions along the Eastern Track. Figure from LeMone et al. (2006)

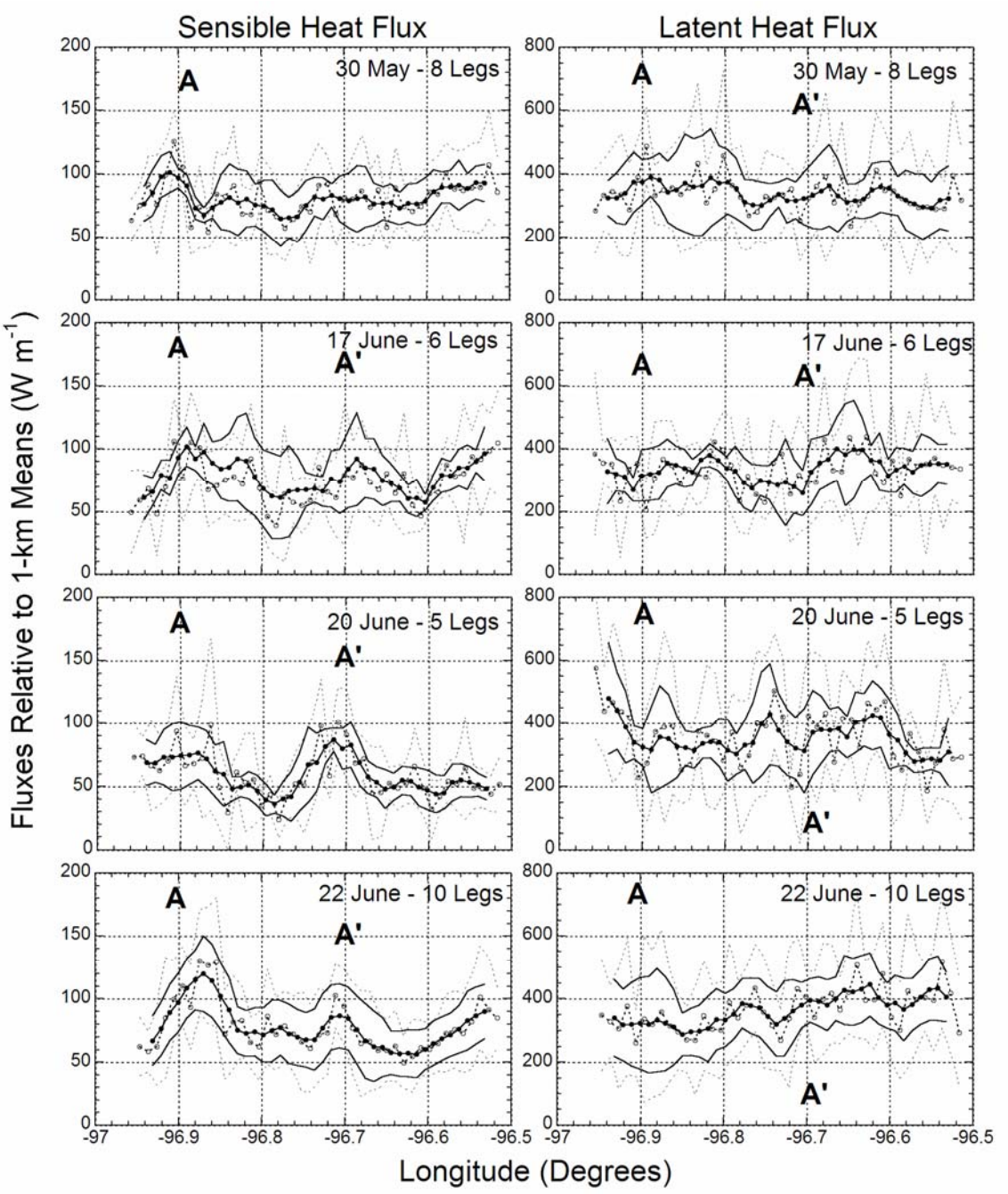

Figure 5. As in Figure 4, but for fluxes calculated relative to 1-km averages, smoothed using a 4-point running mean filter. Figure from LeMone et al. 2006.

As expected, both the magnitudes and standard deviations are smaller for the high-frequency fluxes. Table 1 compares the magnitudes using the two approaches.

Table 1. Comparisons of fluxes averaged from grand average legs. Primes indicate "high frequency" fluxes computed with respect to 1-km block averages, unprimed fluxes are "total" fluxes, computed with respect to flight-leg linear trends.

Date	H	LE	H'	LE'	H'/H	LE'/LE
30 May	91.606	439.77	81.05	338.19	0.88	0.77
17 June	92.78	382.01	73.3	333.12	0.79	0.87
20 June	69.1	421.31	59.07	356.47	0.85	0.85
22 June	92.55	416.68	78.25	363.79	0.85	0.87

b. Error analysis

Table 2 shows estimates of the fractional random error $\sigma^*(F)$ for average total H and LE for each day. We calculated $\sigma^*(F)$ for each leg following Mann and Lenschow (1994) via:

$$\sigma^*(F)_L = \left(\frac{2\lambda_F}{L}\right)^{1/2}\left(\frac{1+r_{w,s}^2}{r_{w,s}^2}\right)^{1/2}, \qquad (2)$$

and then combined the results for all N legs as described in LeMone et al. (2003). In (2), s is a scalar, L is the length of the flight leg (~46 km), λ_F is the integral scale for ws, found from the ws –spectrum as described in Lenschow (1995), and $r_{w,s}$ is the correlation between w and s. Relative to the values in the table, $\sigma^*(F)$ increases by a factor of ~ $(46/4)^{1/2} = 3.39$ for 4-km averages along the grand-average leg.

Table 2. Fractional random uncertainty σ^* in H and LE averaged over all the low-level legs, based on Mann and Lenschow (1994) and Lenschow (1995)

Date	Low Legs	Average H (W m^{-2})	σ^*_H	Average LE (W m^{-2})	σ^*_{LE}
020530	8	94	0.063	380	0.103
020617	6	95	0.086	381	0.106
020620	5	68	0.093	420	0.107
020622	10	92	0.063	423	0.080

References

LeMone, M.A., F. Chen, J. G. Alfieri, M. Tewari, B. Geerts. Q. Miao, R. Grossman, and R. Coulter, 2006: Influence of Land Cover and Soil Moisture on the Horizontal Distribution of Sensible and Latent Heat Fluxes in Southeast Kansas during IHOP_2002 and CASES-97, *J. Hydromet.*, in press. (much of the material comes from this paper)

LeMone, M.A., R.L. Grossman, F. Chen, K. Ikeda, and D. Yates, 2003: Choosing the averaging interval for comparison of observed and modeled fluxes along aircraft transects of a heterogeneous surface. *J. Hydromet.*, **4**, 179-195.

Lenschow, D.H., 1995: Micrometeorological techniques for measuring biosphere-atmosphere trace-gas exchange, Chap. 5, *Biogenic Trace Gases: Measuring Emissions from Soil and Water*, P. Matson and R. Harriss, Eds. Blackwell Science, Cambridge, MA, 126-163.

Mann, J., and D.H. Lenschow, 1994: Errors in airborne flux measurements. *J. Geophys. Res.*, **99**, 14,519-14,526.